Sensors & Actuators: B. Chemical 283 (2019) 426–433

Contents lists available at ScienceDirect

Sensors and Actuators B: Chemical

journal homepage: www.elsevier.com/locate/snb

A multi-dye containing MOF for the ratiometric detection and simultaneous removal of $Cr_2O_7^{2-}$ in the presence of interfering ions

Jounghyun Yoo[a,1], UnJin Ryu[b,1], Woosung Kwon[b,*], Kyung Min Choi[b,*]

[a] Department of Chemical Engineering, Pohang University of Science and Technology (POSTECH), 77 Cheongam-ro, Nam-gu, Pohang, 37673, Republic of Korea
[b] Department of Chemical and Biological Engineering and Institute of Advanced Materials & Systems, Sookmyung Women's University, 100 Cheongpa-ro 47 gil, Yongsan-gu, Seoul, 04310, Republic of Korea

ARTICLE INFO

Keywords:
Molecular dyes/pigments
Metal-organic frameworks
Molecular carrier
Optical sensor
$Cr_2O_7^{2-}$ detection
$Cr_2O_7^{2-}$ removal

ABSTRACT

Among the heavy metals commonly found in wastewater, $Cr_2O_7^{2-}$ is considered the most hazardous due to its high toxicity, carcinogenicity, and mutagenicity. Nevertheless, detection and removal of $Cr_2O_7^{2-}$ remains a serious challenge as it competes with other metal cations and anions in wastewater. Herein, self-calibration of the emission intensities at two different wavelengths was introduced to microporous media to facilitate the ratiometric detection and simultaneous removal of $Cr_2O_7^{2-}$ in the presence of excess interfering ions. Specifically, a multi-dye (7-amino-4-methylcoumarin and resorufin) containing metal-organic framework-801 (Dyes⊂MOF-801) was developed and tested for the detection and removal of $Cr_2O_7^{2-}$ from wastewater. Dyes⊂MOF-801 exhibited accurate detection of $Cr_2O_7^{2-}$ with high sensitivity in the presence of a 260-fold excess of potentially interfering ions. Its maximum removal capacity was 83 mg/g and was achieved within 3 min, even in the presence of excess metal ions and 10-fold excess concentrations of anions. In addition, the residual concentration of $Cr_2O_7^{2-}$ was simultaneously checked using ratiometric detection of Dyes⊂MOF-801, so that the removal of $Cr_2O_7^{2-}$ could be immediately confirmed.

1. Introduction

Heavy metal pollution in wastewater is considered to be one of the most worrisome environmental problems due to the potential adverse effects on human health [1–4]. Since heavy metal ions are highly toxic even at low concentrations and can accumulate in the human body, it is essential to detect and remove them from wastewater. Among heavy metal ions, $Cr_2O_7^{2-}$ is the most dangerous metal ion as it is extremely toxic, carcinogenic, and mutagenic [5–7]. Therefore, the efficient detection and removal of $Cr_2O_7^{2-}$ from aqueous environments is important, but remains challenging as the small amount of $Cr_2O_7^{2-}$ usually co-exists with other heavy metals and anionic counter ions in wastewater. When $Cr_2O_7^{2-}$ is surrounded by a complex environment containing multiple cations and anions, the efficiency of its detection and removal is significantly reduced as the other ions compete for luminescence and adsorption sites. Even if UV absorption of the aqueous solution is used for detecting $Cr_2O_7^{2-}$, it is difficult to obtain reliable signals in the presence of other heavy metal ions as their absorption typically overlapped [8]. Recently, the luminescence properties of various porous materials have been studied to detect $Cr_2O_7^{2-}$ using turn-on and -off mechanisms but are significantly affected by other ions and the surrounding environment [9,10].

Ratiometric detection uses the self-calibration of emission intensities at two different wavelengths which can eliminate, or account for, the interference of the surrounding environment and ambiguities including instrumental efficiency, environmental conditions, and probe concentration [11–13]. Multiple probes encapsulated together within a highly porous material can provide a ratiometric approach for the accurate detection and efficient removal of $Cr_2O_7^{2-}$ in wastewater with minimal environmental effects. In this report, we developed a multi-dye containing metal-organic framework (MOF) for the detection and removal of $Cr_2O_7^{2-}$ from wastewater. Specifically, 7-amino-4-methylcoumarin (coumarin) and resorufin dye molecules were encapsulated within metal-organic frameworks-801 (Dyes⊂MOF-801) [14]. Coumarin and resorufin were chosen because their molecular sizes closely match the pore size (8 Å) of MOF-801 (Fig. S1) [15] and their luminescence properties are significantly affected by the quenching effect of heavy metal ions (Fig. 1). By ratiometrically comparing the maximum emission intensities of coumarin at 440 nm and resorufin at 585 nm, $Cr_2O_7^{2-}$ was clearly identified at a sensitivity 260 times higher than

* Corresponding authors.
E-mail addresses: wkwon@sookmyung.ac.kr (W. Kwon), kmchoi@sookmyung.ac.kr (K.M. Choi).
[1] These authors contributed equally to this work.

https://doi.org/10.1016/j.snb.2018.12.031
Received 2 September 2018; Received in revised form 29 November 2018; Accepted 7 December 2018
Available online 10 December 2018
0925-4005/

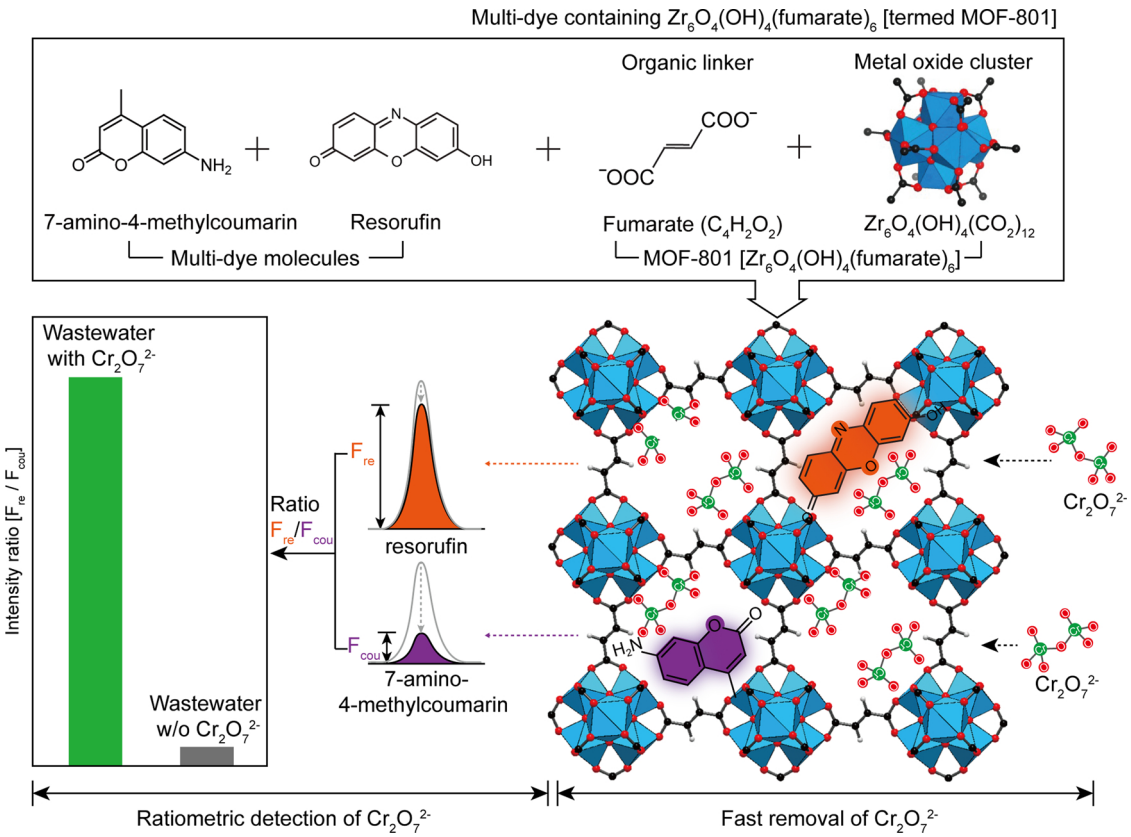

Fig. 1. Schematic of the ratiometric detection and simultaneous removal of $Cr_2O_7^{2-}$ using multi-dye (resorufin and 7-amino-4-methylcoumarin) containing MOF-801.

other ions. The empty pores in MOF-801 efficiently remove $Cr_2O_7^{2-}$ with an equilibrium time of 3 min and an 83 mg/g adsorption capacity. The Dyes⊂MOF-801 s were characterized by transmission electron microscopy (TEM), scanning electron microscopy (SEM), and powder X-ray diffraction (PXRD). The detection and removal of $Cr_2O_7^{2-}$ were confirmed by photoluminescence (PL) and UV–vis absorption spectroscopy.

Many materials including resins, layered double hydroxides, and zeolites have been developed for $Cr_2O_7^{2-}$ detection and/or removal, but lack selectivity, adsorption capacity, and desirable kinetics [16–29]. Alternatively, MOFs combined with luminescent molecules have been applied for the detection and/or removal of $Cr_2O_7^{2-}$ [30–39], but none of the previous studies have encapsulated multiple dyes inside MOFs for ratiometric detection and simultaneous removal with minimal environmental effects.

2. Experimental section

2.1. Materials

NaCl, $NaNO_3$, $NaSO_4$, $Cu(NO_3)_2{\cdot}3H_2O$, $Ga(NO_3)_3{\cdot}H_2O$, $Co(NO_3)_2{\cdot}6H_2O$, $Ni(NO_3)_2{\cdot}6H_2O$, $Zn(NO_3)_2{\cdot}4H_2O$, $Na_2Cr_2O_7$, $Cr(NO_3)_3{\cdot}9H_2O$, $Fe(NO_3)_3{\cdot}9H_2O$, $ZrCl_4$, fumaric acid, acetic acid, *N,N*-dimethylformamide, resorufin, and 7-amino-4-methylcoumarin were purchased from Sigma Aldrich (St. Louis, MO). Triple distilled water was used in all experiments.

2.2. Synthesis of Dyes⊂MOF-801

Stock solutions for each dye solution were prepared to be 0.2 mg/mL of resorufin and 10 mg/mL of 7-amino-4-methylcoumarin in DMF before the synthesis of MOF-801. For the synthesis of Dyes⊂MOF-801, $ZrCl_4$ (33.4 mg, 0.14 mmol) was dissolved in a solution of DMF (4 mL) and acetic acid (0.69 mL) followed by addition of 1 mL of the resorufin stock solution. Separately, fumaric acid (18 mg, 0.15) was dissolved in DMF (4 mL) followed by addition of 1 mL of the coumarin stock solution. These two $ZrCl_4$ and fumaric acid solutions are mixed in a 20 mL vial and then placed in a 90 °C oven for 87 h. In this preparation, $ZrCl_4$ and fumaric acid serve as metal source and organic linker for the construction of MOF-801, respectively. DMF was chosen as solvent as it has high boiling point and high solubility for $ZrCl_4$ and fumaric acid. The role of acetic acid is modulator making competition with the organic linker in the growth of MOF-801 to have high crystallinity. Afterwards, the vial was cooled to room temperature and the solid part was separated with a centrifuge (9000 rpm for 10 min). The solid was then washed with DMF once and with methanol more than three times until no dye is released. After washing, the product was dried in a vacuum oven.

2.3. Characterization

PXRD spectra were obtained using a RIGAKU XRD (Smartlab, Cu-Kα radiation) instrument at 1200 W (40 kV, 30 mA). The scanning condition was 4°/min from 3 to 40° with a silicon holder. The morphology and surface of the MOFs were verified by field emission scanning electron microscopy (FE-SEM, JEM-7600 F, JEOL). The powder sample was dissolved in methanol and dropped directly onto the holder. The PL spectra of sample solutions were obtained using a Jasco FP-8500 fluorometer and the UV–vis absorption spectra recorded using a Scinco S3100 UV–vis spectrometer with QS-grade quartz cuvettes (111-QS, Hellma Analytics). Fourier transform infrared (FTIR) spectroscopy was performed using a Nicolet iS50 FTIR spectrometer (Thermo-Scientific) with KBr pellet method. Gas adsorption analysis was performed using a BELSORP-max automatic volumetric gas adsorption analyzer. The samples were prepared and measured after evacuation at 120 °C for 12 h.

2.4. Ratiometric fluorescence detection of metal ions

3 mM aqueous solutions of metal ions (Na^+, Co^{2+}, Ni^{2+}, Cu^{2+}, Zn^{2+}, Ga^{3+}, Fe^{3+}, and Cr^{3+}) were prepared from their nitrate salts and a 3 mM $Cr_2O_7^{2-}$ solution was prepared from $Na_2Cr_2O_7$. A total of 1 mL of metal ion solution was added to 2 mL of the Dyes⊂MOF-801 solution (3 mg/mL) and mixed in a vial. The PL spectra of each solution were measured under excitation at 350 nm and 570 nm, corresponding to the excitations of 7-amino-4-methylcoumarin and resorufin, respectively. Subsequently, the intensity ratio of the 440 nm (excitation at 350 nm) and 585 nm emissions (excitation at 570 nm) of each metal ion solution were determined. For an intuitive comparison, each intensity and intensity ratio was normalized with respect to water.

2.5. $Cr_2O_7^{2-}$ adsorption test

a. Equilibrium adsorption at different $Cr_2O_7^{2-}$ concentrations

A total of 40 mg of Dyes⊂MOF-801 was weighed and dispersed into an aqueous solution (10 mL) containing different Na_2CrO_7 concentrations (4/15, 4/9, 2/3, 4/3, 2, and 3 mM) with mild stirring for 2 h at room temperature. After 2 h of equilibrium, the mixed solution was pipetted and the Dyes⊂MOF-801 s were removed from the pipetted solutions via centrifugation. Subsequently, each solution was diluted 30 times using deionized water before measuring the UV–vis absorbance. The adsorption capacity of the Dyes⊂MOF-801 was evaluated by measuring the typical absorbance of $Cr_2O_7^{2-}$ at 362 nm using the following equation:

$$Q_e = \frac{C_0 - C_f}{m_{sorbent}} \times V_{solution}$$

Where Q_e represents the adsorption capacity of the Dyes⊂MOF-801; C_0 and C_f represent the concentration of $Cr_2O_7^{2-}$ in the aqueous solution before and after adsorption, respectively; and $m_{absorbent}$ and $V_{solution}$ represent the weight of the sorbent and volume of the $Na_2Cr_2O_7$ aqueous solution, respectively.

b. Adsorption kinetics of $Cr_2O_7^{2-}$ with Dyes⊂MOF-801

A total of 80 mg of Dyes⊂MOF-801 was dispersed in an aqueous solution (20 mL) of Na_2CrO_7 (1.5 mM) with mild stirring at room temperature. The mixed solution was then pipetted at different times (1, 3, 5, 30, 60, and 120 min) and the Dyes⊂MOF-801 s were removed from the pipetted solutions using syringe filters for rapid removal. Subsequently, the amount of $Cr_2O_7^{2-}$ adsorbed to the Dyes⊂MOF-801 at different times were determined by UV absorbance at 362 nm.

2.6. $Cr_2O_7^{2-}$ removal

First, 80 mg of the Dyes⊂MOF-801 were dispersed in 20 mL of $Na_2Cr_2O_7$ solution (2 mM) with mild stirring at room temperature. After 10 min, the Dyes⊂MOF-801 s were separated from the solutions via centrifugation. At each removal step, the absorbance of the $Cr_2O_7^{2-}$ solution at 362 nm and fluorescence intensity ratio (F_{re}/F_{cou}) of the Dyes⊂MOF-801 used in each removal step were measured. This procedure was repeated three times.

3. Results and discussion

MOF-801 was selected because zirconium-based MOFs are chemically stable in aqueous ionic solutions. In a previous study, we showed that MOF-801 can encapsulate molecular dyes in its pores with significant size control [15]. The MOF-801 with dual emission properties was prepared by embedding coumarin (440 nm) and resorufin (585 nm) simultaneously during its synthesis. In a typical synthesis, dye molecules were placed in DMF solution mixture containing $ZrCl_4$, organic linkers, and acetic acid. This mixture was heated to 90 °C for three days to produce a colored precipitate. The product was collected by centrifugation and the reaction solvent was removed. The Dyes⊂MOF-801 was washed with DMF and methanol until no luminescence was detected in the supernatant. The washed product was immersed in methanol for three 24 h periods and dried under vacuum. The product was characterized by PXRD, SEM, and N_2 adsorption. These techniques characterized the crystallinity, permanent porosity, morphology, luminescence properties, and stability of the Dyes⊂MOF-801.

The X-ray diffraction patterns of the prepared Dyes⊂MOF-801 showed sharp diffraction peaks at positions perfectly matched with those of pristine MOF-801 and the simulated structure (Fig. 2a), indicating that Dyes⊂MOF-801 exhibits high crystallinity and the same crystal structure as the pristine sample. In addition, the SEM images show that the Dyes⊂MOF-801 exhibits identical morphology to that of MOF-801 (Fig. S2). The permanent porosity of the Dyes⊂MOF-801 was confirmed by N_2 adsorption measurements in Fig. 2b. The Dyes⊂MOF-801 sample maintains its microporosity allowing the interior adsorption of $Cr_2O_7^{2-}$ but the amount of microporous absorption at pressures up to 0.2 P/P_0 is slightly lower than that of pristine MOF-801 due to the presence of dye molecules. The presence and amount of dye molecules were confirmed by PL spectroscopy (Fig. 2c and d). As shown in Fig. 2c, the emission peaks of coumarin at 440 nm and resorufin at 585 nm were observed in the PL contour map of Dyes⊂MOF-801. When no dye was included in the synthesis procedure, no PL was observed in the MOF-801 solution (Fig. S3). It was also confirmed that no dyes leached out after the washing process. Furthermore, coumarin and resorufin were not encapsulated within UiO-66, which has the same structure but larger pores (12 Å) using an identical synthetic process. These results indicate that both dye molecules were successfully encapsulated without sacrificing their native PL properties. In addition, the amount of coumarin and resorufin within Dyes⊂MOF-801 was independently controlled by differing the amount of each dye in their respective preparation solutions (Fig. 2d). The PL intensity of each dye emitted from Dyes⊂MOF-801 was directly proportional to the amount of corresponding dye in the synthesis solution regardless of the amount of the other dye. We chose a fluorescence intensity ratio of coumarin to resorufin (F_{re}/F_{cou}) of approximately 1.77 for optimal ratiometric detection and the number of coumarin and resorufin dyes in 1 mg of Dyes⊂MOF-801 was determined to be 1.70×10^{16} and 2.51×10^{17}, respectively, using the linear relationship of PL intensity and dye molecule concentration at very low dye concentrations (Fig. S4).

The dual fluorescence emission of Dyes⊂MOF-801 was used for the sensing of metal ions (Fig. 3). When the dyes and heavy metal ions are within several nm, electron transfer from the dye to metal ion occurs, causing fluorescence quenching [40–42]. However, fluorescence quenching is significantly affected by the surrounding environment, a single emission quenching is not efficient for determining $Cr_2O_7^{2-}$ concentrations in unknown aqueous solutions. In this context, we used the dual fluorescence emission of Dyes⊂MOF-801 for ratiometric detection to eliminate interferences from the surrounding environment through self-calibration of emission intensities at two different wavelengths. Dyes⊂MOF-801 was mixed with solutions containing 1 mM of Ga^{3+}, Na^+, Ni^{2+}, Co^{2+}, Zn^{2+}, Cu^{2+}, Cr^{3+}, Fe^{3+}, and $Cr_2O_7^{2-}$ ion in water, and the resulting PL intensities of coumarin and resorufin were measured. As shown in Fig. 3a and b, the degree of fluorescence quenching varied depending on the type of dye and metal ion present in solution. The PL intensity of coumarin was significantly reduced in Fe^{3+} and $Cr_2O_7^{2-}$ solutions while that of resorufin was halved in the $Cr_2O_7^{2-}$ solution comparing with the other metal ion solutions. These results differed significantly from those of from pristine coumarin and resorufin molecules (Fig. S5). The selectivity for different metal ions was significantly enhanced when the coumarin and resorufin were encapsulated in MOF-801. Even if the single emission quenching showed distinct changes when exposed to the metal ions, those changes could not be used to detect target ions in unknown solutions as the overall metal ions concentration also affected PL intensity.

When the dual emission of Dyes⊂MOF-801 was used to obtain the fluorescence intensity ratio of coumarin over resorufin (F_{re}/F_{cou},

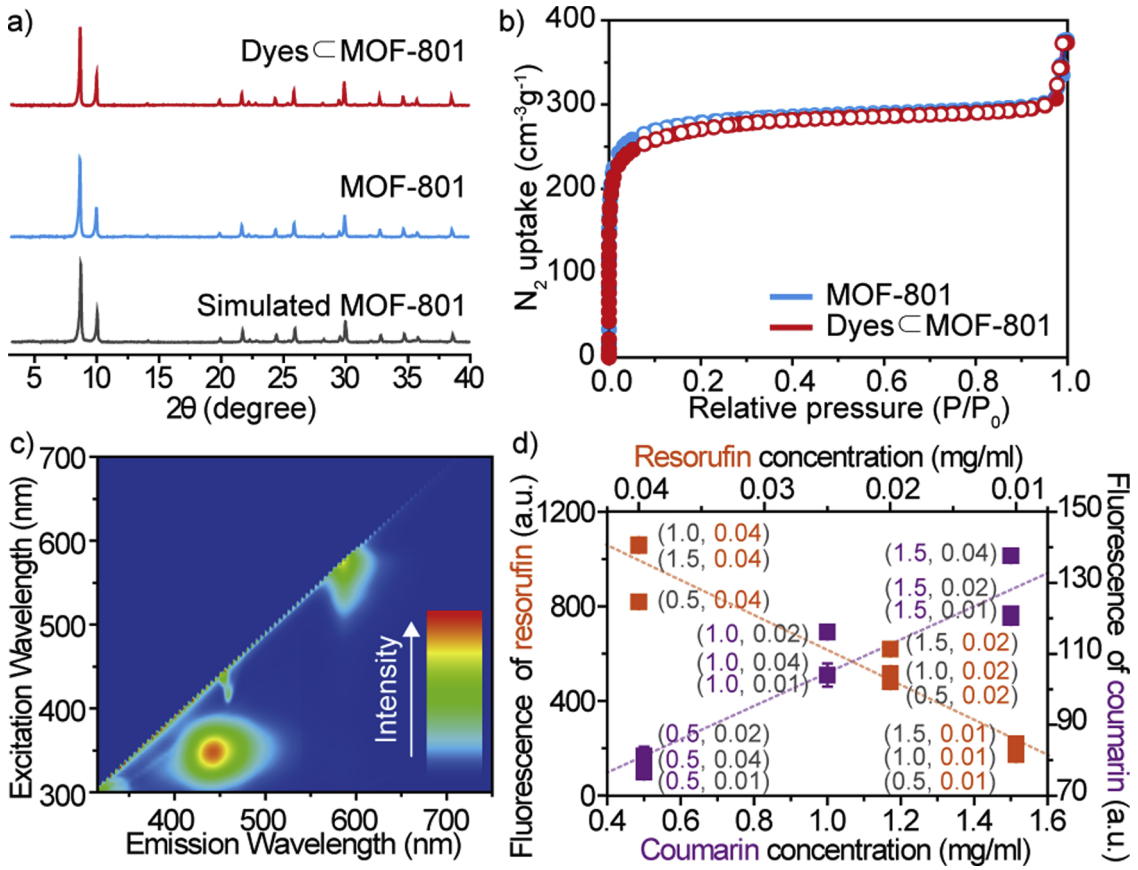

Fig. 2. Characterization of the Dyes⊂MOF-801. (a) XRD patterns of the Dyes⊂MOF-801 and MOF-801. (b) N_2 adsorption of the Dyes⊂MOF-801 and MOF-801. (c) PL contour maps of the Dyes⊂MOF-801 in water. (d) PL intensities of coumarin and resorufin within the Dyes⊂MOF-801 samples synthesized from the prepared solutions with different ratios of the two dyes.

Fig. 3c), the F_{re}/F_{cou} in the $Cr_2O_7^{2-}$ solution was 25 times higher than in the solutions of Ga^{3+}, Na^+, Ni^{2+}, Co^{2+}, Zn^{2+}, Cu^{2+}, and Cr^{3+} and 5 times higher than the Fe^{3+} solution. The power of ratiometric detection was enhanced when $Cr_2O_7^{2-}$ was detected in mixed ion solutions containing all metal ions listed above. To simulate the detection of $Cr_2O_7^{2-}$ in wastewater, reference wastewater was prepared (hereafter denoted as wastewater) containing 1 mM of Ga^{3+}, Na^+, Ni^{2+}, Co^{2+}, Zn^{2+}, Cu^{2+}, Cr^{3+}, Fe^{3+} together, and then various amounts of $Cr_2O_7^{2-}$ were added from 0.1 to 1 mM (Fig. 3d) followed by ratiometric intensity (F_{re}/F_{cou}) comparisons. The ratiometric value (F_{re}/F_{cou} = 7.9) in the 0.1 mM $Cr_2O_7^{2-}$ addition to the wastewater was 2 times higher than that (F_{re}/F_{cou} = 3.1) of the reference wastewater. This is a significant difference as the molar amount of $Cr_2O_7^{2-}$ at 0.1 mM was 260 times less than that of the other ions, considering the wastewater contained 8 mM of metal cations and 18 mM of counter anions. With high concentrations of $Cr_2O_7^{2-}$ added to wastewater, a higher ratiometric intensity was observed (Fig. 3d). When the equivalent amount (1 mM) of $Cr_2O_7^{2-}$ to the each of the other metal ions in the wastewater was added, the ratiometric value (F_{re}/F_{cou} = 54.8) was 18 times higher than that of the reference wastewater. The ratiometric value was directly proportional to the amount of $Cr_2O_7^{2-}$ added to the wastewater, indicating that ratiometric detection can be used to determine the concentration of $Cr_2O_7^{2-}$ in wastewater (Fig. 3e). These results indicate that the ratiometric approach using two dye molecules within MOF-801 can efficiently detect $Cr_2O_7^{2-}$ and can be used for concentration determination in the presence of other possibly interfering ions. It is also confirmed that detection of $Cr_2O_7^{2-}$ can be achieved up to 0.03 mM concentration (Fig. S6).

In MOF-801 [$Zr_6O_4(OH)_4(fumarate)_6$], Zr oxide building units [$Zr_6O_4(OH)_4(CO_2)_{12}$] are used to interconnect linkers [fumarate] with 8 μ_3-oxygen atoms disorderedly occupied by either O^{2-} or OH^- groups [43]. The uneven electrostatic potential at these sites strongly interact with $Cr_2O_7^{2-}$, and empty pores in Dyes⊂MOF-801 easily remove $Cr_2O_7^{2-}$ from aqueous solution. The adsorption capacity of Dyes⊂MOF-801 was studied by measuring its absorbance in different concentrations of $Cr_2O_7^{2-}$ solution (4/15, 4/9, 2/3, 4/3, 2, and 3 mM; 10 mL) after mixing with Dyes⊂MOF-801 (40 mg) for 2 h. It should be noted that Dyes⊂MOF-801 was removed by centrifugation before measuring the absorbance of the solution. Herein, $Cr_2O_7^{2-}$ adsorption was evaluated by measuring the typical absorbance of $Cr_2O_7^{2-}$ at 362 nm. The remaining $Cr_2O_7^{2-}$ in solution was based on the linearly proportional UV–vis absorbance to the amount of $Cr_2O_7^{2-}$ ion at very low concentrations (Fig. S7). The adsorption capacity per gram of Dyes⊂MOF-801 (Q_e) initially increased with increasing concentration of $Cr_2O_7^{2-}$ and became saturated at 400 ppm (Fig. 4a). The adsorption isotherm was well fitted by the Langmuir model (Figs. 4a and S8). From the Langmuir model, the fitting results indicated that the maximum adsorption capacity was 83 mg of $Cr_2O_7^{2-}$ per gram of Dyes⊂MOF-801 (83 mg/g).

For a more detailed description of the overall process, the adsorption kinetics of $Cr_2O_7^{2-}$ by Dyes⊂MOF-801 was studied at different adsorption times (Fig. 4b). In addition, the UV–vis absorbance at 362 nm was converted to adsorption capacity at the different times (Q_t) of interaction with Dyes⊂MOF-801. In these experiments, 324 ppm of $Cr_2O_7^{2-}$ in 20 mL of aqueous solution and 80 mg of Dyes⊂MOF-801 were used for kinetic determination. As shown in Fig. 4b, the $Cr_2O_7^{2-}$ adsorption by Dyes⊂MOF-801 reached equilibrium in 3 min, which is considerably faster than other $Cr_2O_7^{2-}$ sorbents, including other types of MOFs [44,45].

To characterize the selective adsorption of $Cr_2O_7^{2-}$ by Dyes⊂MOF-

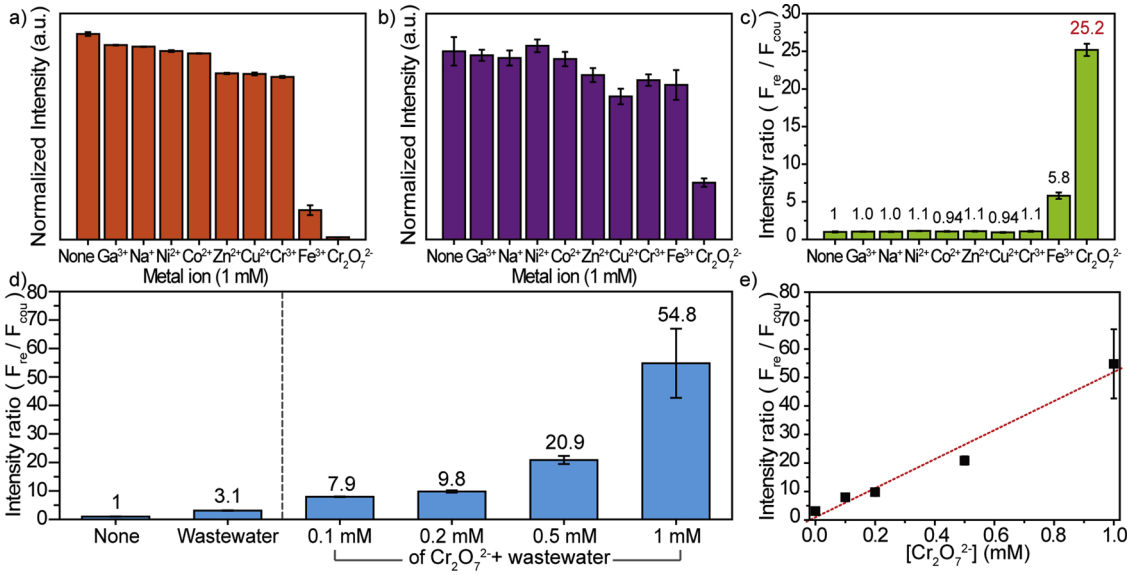

Fig. 3. Histograms of the normalized fluorescence intensity changes of Dyes⊂MOF-801 (a) at 440 nm with 350 nm excitation and (b) at 585 nm with 570 nm excitation. (c) Fluorescence intensity ratio (F_{re}/F_{cou}) changes in the presence of different metal ions (1 mM). (d) Fluorescence intensity ratio (F_{re}/F_{cou}) of Dyes⊂MOF-801 in wastewater with or without added $Cr_2O_7^{2-}$ (0.1, 0.2, 0.5, 1 mM). (e) Fluorescence intensity ratio (F_{re}/F_{cou}) of Dyes⊂MOF-801 as a function of $Cr_2O_7^{2-}$ added to the wastewater.

801 in the presence of potentially interfering metal ions, $Cr_2O_7^{2-}$ removal from wastewater was tested by measuring UV–vis absorbance. As shown in Fig. 4c, after the removal process, the UV–vis absorbance of the wastewater was similar to that of the control wastewater without $Cr_2O_7^{2-}$, especially at the typical absorbance of $Cr_2O_7^{2-}$ (362 nm), implying that $Cr_2O_7^{2-}$ was selectively removed. To ensure that other metal ions were not removed in the adsorption process, the removal experiment of the wastewater without $Cr_2O_7^{2-}$ was also conducted (Fig. S9). When the wastewater did not contain $Cr_2O_7^{2-}$, the UV–vis absorbance was similar after the same removal experiment, indicating that other metal ions are not significantly affected by the adsorption. The selective adsorption of $Cr_2O_7^{2-}$ in the presence of various anions was also studied under 10-fold excess concentrations of Cl-, NO_3-, and SO_4^{2-} (Fig. 4d). Cl-, NO_3-, SO_4^{2-} ions are well-known as competitive anions to $Cr_2O_7^{2-}$ adsorption, but the adsorption capacity for $Cr_2O_7^{2-}$ by Dyes⊂MOF-801 was maintained regardless of the addition of other anions. Also, the ratiometric value of Dyes⊂MOF-801 was measured in the presence of 1 mM of Cl-, NO^{3-}, CO_3^{2-}, SO_4^{2-}, PO_4^{3-}, and citrate using their sodium salts (Fig. S10). The results show that interference of anion has negligible effect on the detection of $Cr_2O_7^{2-}$.

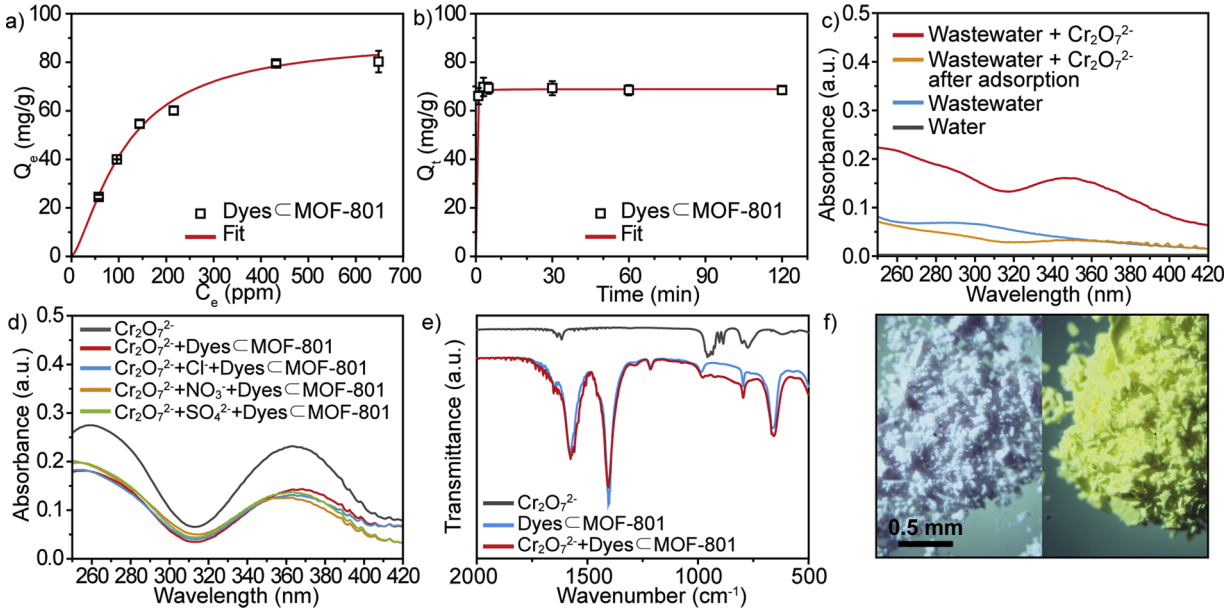

Fig. 4. (a) Equilibrium $Cr_2O_7^{2-}$ adsorption for Dyes⊂MOF-801. The solid line represents fitting of the data with the Langmuir model. (b) Adsorption kinetics of $Cr_2O_7^{2-}$ with Dyes⊂MOF-801. (c) UV–vis spectra of the wastewater with or without $Cr_2O_7^{2-}$ before and after adsorption with Dyes⊂MOF-801. (d) Selectivity adsorption test of $Cr_2O_7^{2-}$ by Dyes⊂MOF-801 after addition of 10-fold higher concentrations of Cl-, NO_3-, SO_4^{2-}. (e) FT-IR spectra of $Na_2Cr_2O_7$ and Dyes⊂MOF-801 before and after $Cr_2O_7^{2-}$ adsorption. (f) Color change of Dyes⊂MOF-801 before and after $Cr_2O_7^{2-}$ adsorption.

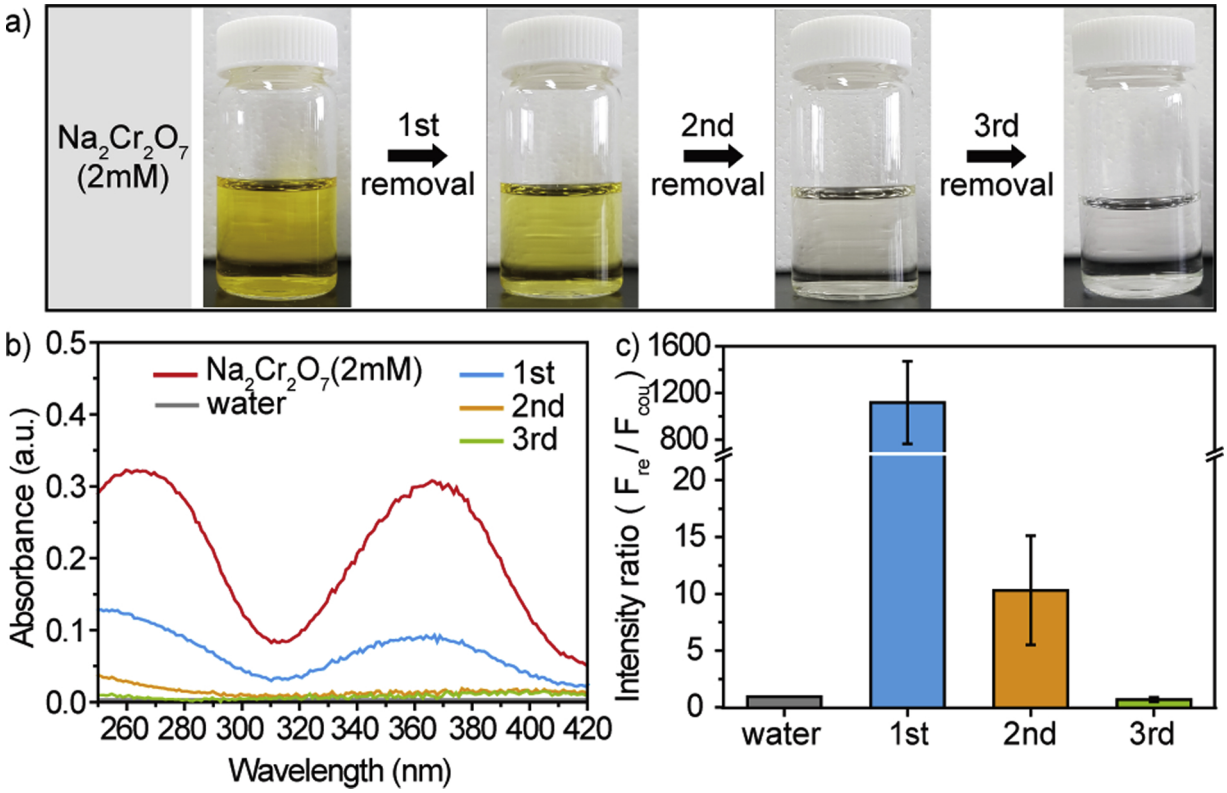

Fig. 5. (a) Color change of the $Cr_2O_7^{2-}$ solution during the repeated ion removal process. (b) UV–vis spectra of the $Cr_2O_7^{2-}$ solution before and after the repeated removal process. (c) Fluorescence intensity ratio (F_{re}/F_{cou}) of the Dyes⊂MOF-801 used in each removal step.

Adsorption of $Cr_2O_7^{2-}$ was confirmed by IR spectroscopy of the Dyes⊂MOF-801 and the results are shown in Fig. 4e. The spectra of the Dyes⊂MOF-801 after adsorption of $Cr_2O_7^{2-}$ maintained the main peaks observed for the MOF-801 structure at 1581, 1401, and 658 cm^{-1}. Furthermore, the sharp band at 1636 cm^{-1} and broad band between 980 and 738 cm^{-1} corresponding to $Cr_2O_7^{2-}$ were retained even after three washing cycles. Additionally, the N_2 adsorption of the sample after $Cr_2O_7^{2-}$ removal was reduced by more than half of the original Dyes⊂MOF-801 and the surface area decreased from 1042.8 to 392 $m^2 g^{-1}$ (Fig. S11). These result indicates that $Cr_2O_7^{2-}$ is captured and remained inside of the micropores of Dyes⊂MOF-801. As shown in Fig. 4f, the color of Dyes⊂MOF-801, originally pinkish-white, changed to yellow after adsorption of $Cr_2O_7^{2-}$. In addition, the yellow color of Dyes⊂MOF-801 after adsorption did not return to its original state even after washing with water and ethanol 3 times, indicating that $Cr_2O_7^{2-}$ was adsorbed to the Dyes⊂MOF-801 by strong interactions.

The simultaneous $Cr_2O_7^{2-}$ detection and removal by Dyes⊂MOF-801 was examined in 20 mL of $Na_2Cr_2O_7$ solution (2 mM) through repeated removal processes using 80 mg of Dyes⊂MOF-801 in each removal step (Fig. 5). As shown in Fig. 5a, the color of the $Cr_2O_7^{2-}$ solution, initially deep yellow, gradually disappeared with repeated removal processes, becoming transparent after only three cycles. From the UV–vis spectra (Fig. 5b), it is clear that the absorption of the solution at 362 nm gradually decreased with the number of removal cycles, and finally becomes similar to that of water. From the absorbance at 362 nm, the concentration of $Cr_2O_7^{2-}$ was determined to be 56 μM after three removal steps, which corresponds to approximately 1/37 of the initial concentration. The removal of $Cr_2O_7^{2-}$ in solution was simultaneously confirmed by the ratiometric detection of Dyes⊂MOF-801. As shown in Fig. 5c, the fluorescence intensity ratio of Dyes⊂MOF-801 used in the first removal process was several hundred times larger than the control value. As the removal process was repeated, the fluorescence intensity ratio decreased gradually and finally became even lower than the value of water after three removal steps. The results indicated that $Cr_2O_7^{2-}$ removal can be confirmed immediately by measuring the fluorescence of Dyes⊂MOF-801 using ratiometric detection.

4. Conclusions

In this study, we encapsulated coumarin and resorufin dye molecules in MOF-801 for ratiometric detection and simultaneous removal of $Cr_2O_7^{2-}$ from wastewater. The ratiometric detection of Dyes⊂MOF-801 enabled the detection of $Cr_2O_7^{2-}$ even in the presence of a 260-fold excess of interfering ions by self-calibration of two different fluorescence emissions. The MOF pores effectively removed $Cr_2O_7^{2-}$ in 3 min with an 83 mg/g of adsorption capacity. Moreover, Dyes⊂MOF-801 exhibited selective removal of $Cr_2O_7^{2-}$ even in the presence of excess interfering metal ions and anions. The Dyes⊂MOF-801 also work as an indicator to measure the residual concentration of $Cr_2O_7^{2-}$, so that the removal of $Cr_2O_7^{2-}$ could be immediately confirmed. The approach developed herein combining ratiometric detection from multiple dyes and the removal capabilities of porous MOF show great potential for solving heavy metal pollution problems by selective detection and removal from actual wastewater.

Acknowledgements

This study was supported by the Basic Science Research Programs of the National Research Foundation of Korea (NRF, 2016R1C1B1010781, 2016R1C1B1011830, and 2009-0082580). W. K. and J. Y. were supported by the KIST Institutional Program (2E28200-18-018). K.M.C and U.R. were further supported by the Sookmyung Women's University Research Grant (1-1703-2034) and NRF-2017-Global Ph.D. Fellowship Program (2017H1A2A1044712), respectively.

Appendix A. Supplementary data

Supplementary material related to this article can be found, in the online version, at doi:https://doi.org/10.1016/j.snb.2018.12.031.

References

[1] C.J. Williams, D. Aderhold, R.G.J. Edyvean, Comparison between biosorbents for the removal of metal ions from aqueous solutions, Water Res. 32 (1998) 216–224, https://doi.org/10.1016/S0043-1354(97)00179-6.
[2] K. Kadirvelu, K. Thamaraiselvi, C. Namasivayam, Removal of heavy metals from industrial wastewaters by adsorption onto activated carbon prepared from an agricultural solid waste, Bioresour. Technol. 76 (2001) 63–65, https://doi.org/10.1016/S0960-8524(00)00072-9.
[3] C. Blöcher, J. Dorda, V. Mavrov, H. Chmiel, N.K. Lazaridis, K.A. Matis, Hybrid flotation-membrane filtration process for the removal of heavy metal ions from wastewater, Water Res. 37 (2003) 4018–4026, https://doi.org/10.1016/S0043-1354(03)00314-2.
[4] W.S. Wan Ngah, M.A.K.M. Hanafiah, Removal of heavy metal ions from wastewater by chemically modified plant wastes as adsorbents: a review, Bioresour. Technol. 99 (2008) 3935–3948, https://doi.org/10.1016/j.biortech.2007.06.011.
[5] J. Barnhart, Chromium chemistry and implications for environmental fate and toxicity, J. Soil. Contam. 6 (1997) 561–568, https://doi.org/10.1080/15320389709383589.
[6] A. Zhitkovich, Importance of chromium-DNA adducts in mutagenicity and toxicity of chromium (VI), Chem. Res. Toxicol. 18 (2005) 3–11, https://doi.org/10.1021/tx049774+.
[7] M. Costa, C.B. Klein, Toxicity and carcinogenicity of chromium compounds in humans, Crit. Rev. Toxicol. 36 (2006) 155–163, https://doi.org/10.1080/10408440500534032.
[8] R.P. Buck, S. Singhadeja, L.B. Rogers, Ultraviolet absorption spectra of some inorganic ions in aqueous solutions, Anal. Chem. 26 (1954) 1240–1242, https://doi.org/10.1021/ac60091a051.
[9] Y. Su, Y. Wang, X. Li, X. Li, R. Wang, Imidazolium-based porous organic polymers: anion exchange-driven capture and luminescent probe of $Cr_2O_7^{2-}$, ACS Appl. Mater. Interfaces 8 (2016) 18904–18911, https://doi.org/10.1021/acsami.6b05918.
[10] Y. Wang, H. Zhao, X. Li, R. Wang, A durable luminescent ionic polymer for rapid detection and efficient removal of toxic $Cr_2O_7^{2-}$, J. Mater. Chem. A 4 (2016) 12554–12560, https://doi.org/10.1039/C6TA03516G.
[11] L. Yuan, W. Lin, Y. Yang, A ratiometric fluorescent probe for specific detection of cysteine over homocysteine and glutathione based on the drastic distinction in the kinetic profiles, Chem. Commun. 47 (2011) 6275–6277, https://doi.org/10.1039/c1cc11316j.
[12] X. Zhang, Y. Xiao, X. Qian, A ratiometric fluorescent probe based on FRET for imaging Hg^{2+} ions in living cells, Angew. Chem. Int. Ed. 47 (2008) 8025–8029, https://doi.org/10.1002/anie.200803246.
[13] Y. Chen, C. Zhu, Z. Yang, J. Chen, Y. He, Y. Jiao, W. He, L. Qiu, J. Cen, Z. Guo, A ratiometric fluorescent probe for rapid detection of hydrogen sulfide in mitochondria, Angew. Chem. Int. Ed. 52 (2013) 1688–1691, https://doi.org/10.1002/anie.201207701.
[14] G. Wißmann, A. Schaate, S. Lilienthal, I. Bremer, A.M. Schneider, P. Behrens, Modulated synthesis of Zr-fumarate MOF, Microporous Mesoporous Mater. 152 (2012) 64–70, https://doi.org/10.1016/j.micromeso.2011.12.010.
[15] U. Ryu, J. Yoo, W. Kwon, K.M. Choi, Tailoring nanocrystalline metal-organic frameworks as fluorescent dye carriers for bioimaging, Inorg. Chem. 56 (2017) 12859–12865, https://doi.org/10.1021/acs.inorgchem.7b01684.
[16] J.B. Qu, S.H. Li, Y.L. Xu, Y. Liu, J.G. Liu, Inherently fluorescent polystyrene microspheres as a fluorescent probe for highly sensitive determination of chromium (VI) and mercury (II) ions, Sens. Actuators B 272 (2018) 127–134, https://doi.org/10.1016/j.snb.2018.05.087.
[17] L. Zou, Y. Wen, H. Zhang, J. Chai, X. Duan, L. Shen, G. Zhang, J. Xu, Highly sensitive fluorescent sensor based on electrosynthesized poly(Fmoc-L-serine) enables ultra-trace analysis of $Cr_2O_7^{2-}$ in water and agro-product samples, Sens. Actuators B 277 (2018) 394–400, https://doi.org/10.1016/j.snb.2018.09.046.
[18] S.V. Prasanna, P. Vishnu Kamath, Chromate uptake characteristics of the pristine layered double hydroxides of Mg with Al, Solid State Sci. 10 (2008) 260–266, https://doi.org/10.1016/j.solidstatesciences.2007.09.023.
[19] N. Li, Y. Tian, J. Zhao, J. Zhang, J. Zhang, W. Zuo, Y. Ding, Efficient removal of chromium from water by Mn_3O_4@ZnO/Mn_3O_4 composite under simulated sunlight irradiation: synergy of photocatalytic reduction and adsorption, Appl. Catal., B 214 (2017) 126–136, https://doi.org/10.1016/j.apcatb.2017.05.041.
[20] Z. Lv, C. Liang, J. Cui, Y. Zhang, S. Xu, A facile route for the synthesis of mesoporous melamine-formaldehyde resins for hexavalent chromium removal, RSC Adv. 5 (2015) 18213–18217, https://doi.org/10.1039/c4ra16866f.
[21] J.A. Korak, R. Huggins, M. Arias-Paic, Regeneration of pilot-scale ion exchange columns for hexavalent chromium removal, Water Res. 118 (2017) 141–151, https://doi.org/10.1016/j.watres.2017.03.018.
[22] N. Rahbar, Z. Salehnezhad, A. Hatamie, A. Babapour, Graphitic carbon nitride nanosheets as a fluorescent probe for chromium speciation, Microchim. Acta 185 (2018), https://doi.org/10.1007/s00604-017-2615-3.
[23] W. Daoud, T. Ebadi, A. Fahimifar, Optimization of hexavalent chromium removal from aqueous solution using acid-modified granular activated carbon as adsorbent through response surface methodology, Korean J. Chem. Eng. 32 (2015) 1119–1128, https://doi.org/10.1007/s11814-014-0337-3.
[24] M. Ahmadi, E. Kouhgardi, B. Ramavandi, Physico-chemical study of dew melon peel biochar for chromium attenuation from simulated and actual wastewaters, Korean J. Chem. Eng. 33 (2016) 2589–2601, https://doi.org/10.1007/s11814-016-0135-1.
[25] N.M. Mubarak, R.K. Thines, N.R. Sajuni, E.C. Abdullah, J.N. Sahu, P. Ganesan, N.S. Jayakumar, Adsorption of chromium (VI) on functionalized and non-functionalized carbon nanotubes, Korean J. Chem. Eng. 31 (2014) 1582–1591, https://doi.org/10.1007/s11814-014-0101-8.
[26] R. Jayakumar, M. Rajasimman, C. Karthikeyan, Sorption and desorption of hexavalent chromium using a novel brown marine algae sargassum myriocystum, Korean J. Chem. Eng. 32 (2015) 2031–2046, https://doi.org/10.1007/s11814-015-0036-8.
[27] M. Noroozifar, M. Khorasani-Motlagh, M.N. Gorgij, H.R. Naderpour, Adsorption behavior of Cr (VI) on modified natural zeolite by a new bolaform N,N,N,N′,N′,N′-hexamethyl-1,9-nonanediammonium dibromide reagent, J. Hazard. Mater. 155 (2008) 566–571, https://doi.org/10.1016/j.jhazmat.2007.11.094.
[28] Y. Lu, B. Jiang, L. Fang, F. Ling, J. Gao, F. Wu, X. Zhang, High performance NiFe layered double hydroxide for methyl orange dye and Cr (VI) adsorption, Chemosphere 152 (2016) 415–422, https://doi.org/10.1016/j.chemosphere.2016.03.015.
[29] Y. Xing, X. Chen, D. Wang, Electrically regenerated ion exchange for removal and recovery of Cr (VI) from wastewater, Environ. Sci. Technol. 41 (2007) 1439–1443, https://doi.org/10.1021/es061499l.
[30] J. Xiao, J. Liu, X. Gao, G. Ji, D. Wang, Z. Liu, A multi-chemosensor based on Zn-MOF: ratio-dependent color transition detection of Hg (II) and highly sensitive sensor of Cr (VI), Sens. Actuators B 269 (2018) 164–172, https://doi.org/10.1016/j.snb.2018.04.129.
[31] M.M.H. Khalil, A. Shahat, A. Radwan, M.F. El-Shahat, Colorimetric determination of Cu (II) ions in biological samples using metal-organic framework as scaffold, Sens. Actuators B 233 (2016) 272–280, https://doi.org/10.1016/j.snb.2016.04.079.
[32] X.-X. Wu, H.-R. Fu, M.-L. Han, Z. Zhou, L.F. Ma, Tetraphenylethylene immobilized metal-organic frameworks: highly sensitive fluorescent sensor for the detection of $Cr_2O_7^{2-}$ and nitroaromatic explosives, Cryst. Growth Des. 17 (2017) 6041–6048, https://doi.org/10.1021/acs.cgd.7b01155.
[33] Z.J. Lin, H.Q. Zheng, H.Y. Zheng, L.P. Lin, Q. Xin, R. Cao, Efficient capture and effective sensing of $Cr_2O_7^{2-}$ from water using a zirconium metal-organic framework, Inorg. Chem. 56 (2017) 14178–14188, https://doi.org/10.1021/acs.inorgchem.7b02327.
[34] T. He, Y. Zhang, X. Kong, J. Yu, X. Lv, Y. Wu, Z. Guo, J. Li, Zr (IV)-based metal-organic framework with T-shaped ligand: unique structure, high stability, selective detection, and rapid adsorption of $Cr_2O_7^{2-}$ in water, ACS Appl. Mater. Interfaces 10 (2018) 16650–16659, https://doi.org/10.1021/acsami.8b03987.
[35] R.C. Gao, F.S. Guo, N.N. Bai, Y.L. Wu, F. Yang, J.Y. Liang, Z.J. Li, Y.Y. Wang, Two 3D isostructural Ln (III)-MOFs: displaying the slow magnetic relaxation and luminescence properties in detection of nitrobenzene and $Cr_2O_7^{2-}$, Inorg. Chem. 55 (2016) 11323–11330, https://doi.org/10.1021/acs.inorgchem.6b01899.
[36] X. Sun, S. Yao, C. Yu, G. Li, C. Liu, Q. Huo, Y. Liu, An ultrastable Zr-MOF for fast capture and highly luminescence detection of $Cr_2O_7^{2-}$ simultaneously in an aqueous phase, J. Mater. Chem. A 6 (2018) 6363–6369, https://doi.org/10.1039/c8ta01060a.
[37] W. Liu, Y. Wang, Z. Bai, Y. Li, Y. Wang, L. Chen, L. Xu, J. Diwu, Z. Chai, S. Wang, Hydrolytically stable luminescent cationic metal organic framework for highly sensitive and selective sensing of chromate anions in natural water systems, ACS Appl. Mater. Interfaces 9 (2017) 16448–16457, https://doi.org/10.1021/acsami.7b03914.
[38] X. Li, H. Xu, F. Kong, R. Wang, A cationic metal-organic framework consisting of nanoscale cages: capture, separation, and luminescent probing of $Cr_2O_7^{2-}$ through a single-crystal to single-crystal process, Angew. Chem. Int. Ed. 52 (2013)

13769–13773, https://doi.org/10.1002/anie.201307650.
[39] S. Rapti, D. Sarma, S.A. Diamantis, E. Skliri, G.S. Armatas, A.C. Tsipis, Y.S. Hassan, M. Alkordi, C.D. Malliakas, M.G. Kanatzidis, T. Lazarides, J.C. Plakatouras, M.J. Manos, All in one porous material: exceptional sorption and selective sensing of hexavalent chromium by using a Zr^{4+} MOF, J. Mater. Chem. A 5 (2017) 14707–14719, https://doi.org/10.1039/c7ta04496h.
[40] H. Masuhara, H. Shioyama, T. Saito, K. Hamada, S. Yasoshima, N. Mataga, Fluorescence quenching mechanism of aromatic hydrocarbons by closed-shell heavy metal ions in aqueous and organic solutions, J. Phys. Chem. 88 (1984) 5868–5873, https://doi.org/10.1021/j150668a026.
[41] E. Dulkeith, A.C. Morteani, T. Niedereichholz, T.A. Klar, J. Feldmann, S.A. Levi, F.C.J.M. van Veggel, D.N. Reinhoudt, M. Möller, D.I. Gittins, Fluorescence quenching of dye molecules near gold nanoparticles: radiative and nonradiative effects, Phys. Rev. Lett. 89 (2002) 203002, https://doi.org/10.1103/PhysRevLett.89.203002.
[42] I.K. Kandela, R.M. Albrecht, Fluorescence quenching by colloidal heavy metals nanoparticles: implications for correlative fluorescence and electron microscopy studies, Scanning 29 (2007) 152–161, https://doi.org/10.1002/sca.20055.
[43] H. Furukawa, F. Gándara, Y.-B. Zhang, J. Jiang, W.L. Queen, M.R. Hudson, O.M. Yaghi, Water adsorption in porous metal-organic frameworks and related materials, J. Am. Chem. Soc. 136 (2014) 4369–4381, https://doi.org/10.1021/ja500330a.
[44] J. Li, X. Wang, G. Zhao, C. Chen, Z. Chai, A. Alsaedi, T. Hayat, X. Wang, Metal-organic framework-based materials: superior adsorbents for the capture of toxic and radioactive metal ions, Chem. Soc. Rev. 47 (2018) 2322–2356, https://doi.org/10.1039/c7cs00543a.
[45] S. Sen Gupta, K.G. Bhattacharyya, Kinetics of adsorption of metal ions on inorganic materials: a review, Adv. Colloid Interface Sci. 162 (2011) 39–58, https://doi.org/10.1016/j.cis.2010.12.004.

Jounghyun Yoo received his B.S. in Chemical Engineering from Pohang University of Science and Technology (POSTECH). He is currently pursuing his Ph.D. in Chemical Engineering at POSTECH. His research interests focus on optical properties of biocompatible nanomaterials in the fields of optoelectronics, biomedical imaging, and therapy.

UnJin Ryu She received the B. S. degree in Chemistry from the Sungshin Women's University in 2014 and master's degree in Engineering from Korea Advanced Institute of Science and Technology in 2016. She is currently pursuing her Ph.D. in Chemical and Biological Engineering at Sookmyung Women's University. She is interested in metal-organic frameworks, storage system, biological application and green energy.

Woosung Kwon received his B.S. in Chemical Engineering with a minor in Physics (2010) and Ph.D. in Chemical Engineering (2013) from Pohang University of Science and Technology (POSTECH). After postdoctoral research at Stanford University, he joined the faculty of Sookmyung Women's University, where he is now serving as an assistant professor of chemical and biological engineering. His research interests include (1) development of functional, biocompatible nanomaterials for theragnostic and optoelectronic applications, (2) advancement of functionality of nanomaterials through atomic doping and molecular conjugation, and (3) study of the effect of nanomaterials on physiological biochemical processes in living organisms to address nanotoxicological issues.

Kyung Min Choi received a B.S. in Inorganic Materials Engineering from Kyungpook National University in 2007 and a Ph.D. in Materials Science and Engineering from KAIST in 2012. He did postdoctoral research at University of California, Berkeley before joining the faculty in the Department of Chemical and Biological Engineering at the Sookmyung Women's University in 2016.